Published in final edited form as:
Brain Res. 2014 March 10; 1551: 45–58. doi:10.1016/j.brainres.2014.01.013.

INVOLVEMENT OF P38 MAPK IN REACTIVE ASTROGLIOSIS INDUCED BY ISCHEMIC STROKE

Gourav Roy Choudhury[a], **Myoung-Gwi Ryou**[a], **Ethan Poteet**[a], **Yi Wen**[a], **Runlian He**[a], **Fen Sun**[a], **Fang Yuan**[b], **Kunlin Jin**[a], and **Shao-Hua Yang**[a,b,*]

[a]Department of Pharmacology and Neuroscience, University of North Texas Health Science Center at Fort Worth, 3500 Camp Bowie Blvd, Fort Worth, 76107, Texas, USA

[b]Department of Neurosurgery, Beijing Tiantan Hospital, Beijing Neurosurgical Institute, Capital Medical University, Beijing, 100050, China

Abstract

Reactive astrogliosis is an essential feature of astrocytic response to all forms of central nervous system (CNS) injury and disease, which may benefit or harm surrounding neural and non-neural cells. Despite extensive study, its molecular triggers remain largely unknown in term of ischemic stroke. In the current study we investigated the role p38 mitogen-activated protein kinase (MAPK) in astrogliosis both in vitro and in vivo. In a mouse model of middle cerebral artery occlusion (MCAO), p38 MAPK activation was observed in the glia scar area, along with increased glial fibrillary acidic protein (GFAP) expression. In primary astrocyte cultures, hypoxia and scratch injury-induced astrogliosis was attenuated by both p38 inhibition and knockout of p38 MAPK. In addition, both knockout and inhibition of p38 MAPK also reduced astrocyte migration, but did not affect astrocyte proliferation. In a mouse model of permanent MCAO, no significant difference in motor function recovery and lesion volume was observed between conditional GFAP/p38 MAPK knockout mice and littermates. While a significant reduction of astrogliosis was observed in the GFAP/p38 knockout mice compared with the littermates. Our findings suggest that p38 MAPK signaling pathway plays an important role in the ischemic stroke-induced astrogliosis and thus may serve as a novel target to control glial scar formation.

Keywords

p38 MAPK; astrocytes; astrogliosis; glial fibrillary acidic protein; stroke; ischemia

*Corresponding author at: University of North Texas Health Science Center, Department of Pharmacology and Neuroscience 3500 Camp Bowie Boulevard, Fort Worth, TX 76107, United States. Tel.: +1 817 735 2250; fax: +1 817 735 2091. shaohua.yang@unthsc.edu.

Disclosure/Conflict of Interest:
None.

1. Introduction

Despite the perception as an immune privilege site, immune responses in the central nervous system (CNS) are common which can be mediated by resident microglia, astrocyte and infiltrating peripheral immune cells (Ransohoff and Brown, 2012). Astrocytes are the most abundant cell type in the CNS and respond to all forms of insults by a process commonly referred as reactive astrogliosis characterized as hypertrophy of cellular processes and upregulation of intermediate filament proteins as glial fibrillary acidic protein (GFAP) (Sofroniew, 2009). Compelling evidence has indicated that reactive astrogliosis is not simply an all-or-none phenomenon, but rather a finely tuned continuum of molecular, cellular, and functional changes that range from subtle alternations in gene expression to scar formation. Studies indicate that reactive astrogliosis may exert both beneficial and detrimental effects in a context-dependent manner regulated by specific molecular signaling cascades, including signal transducers and activators of transcription (STAT3), nuclear factor kappaB (NFκB), and mTOR signaling after spinal cord injury (Brambilla et al., 2005; Codeluppi et al., 2009; Herrmann et al., 2008; Sofroniew, 2009).

In term of ischemic stroke, reactive astrogliosis with compact glial scar formation may protect the surrounding healthy brain from exposure to the toxic elements and cellular debris in the infarct area. On the other hand, it may also impede axonal regeneration, which, in turn, hinders the functional recovery process. Surprisingly, our knowledge of astrocyte pathophysiology and its underlying mechanisms of glial scar formation after ischemic stroke are extremely limited. A better understanding of signaling mechanisms that regulate specific aspects of reactive astrogliosis after ischemic stroke may lead to novel pharmacological strategies to attenuate detrimental aspects of astrogliosis, enhance neural repair processes, and improve stroke recovery.

p38 Mitogen-activated protein kinase (p38 MAPK) was first isolated as a 38-kDa protein that was rapidly tyrosine phosphorylated in response to lipopolysaccharide stimulation. To date, four splice variants of the p38 family have been identified: p38α, p38β, p38γ, and p38δ. The main biological response of p38 activation involves the production and activation of inflammatory mediators to initiate leukocyte recruitment and activation (Kumar et al., 2003). Of the four p38 variants, p38α is the best characterized and perhaps the most physiologically relevant kinase involved in inflammatory responses (Kumar et al., 2003). The activation of the p38 MAPK pathway plays essential roles in the production of pro-inflammatory cytokines such as TNFα, IL-1β, and IL-6. Currently, the majority of studies favor that these cytokines act as perpetrators in the CNS injury (Wang and Shuaib, 2002). In addition, increasing evidence has indicated that p38 plays a role in many other biological functions in the CNS (Takeda and Ichijo, 2002). Activation of p38 signaling after ischemic stroke has been identified in neuron, astrocyte and microglia (Ferrer et al., 2003; Krupinski et al., 2003; Nozaki et al., 2001; Piao et al., 2002). Furthermore, inhibition of p38 activation has been found to provide protection in experimental ischemic stroke models (Barone et al., 2001; Legos et al., 2001; Legos et al., 2002; Nito et al., 2008; Nozaki et al., 2001; Piao et al., 2003; Strassburger et al., 2008). Thus, p38 MAPK has been recognized as a potential therapeutic target for ischemic stroke. In the current study, we evaluated the role of p38 MAPK signaling in astrogliosis after ischemic stroke. Using primary astrocyte culture and

mouse model middle cerebral artery occlusion (MCAO) models, we demonstrated that inactivation of p38 MAPK signaling abrogate ischemic stroke-induced astrocyte reactivation.

2. Results

2.1. Ischemic stroke induces GFAP and p38 expression in the peri-infarct area

To investigate the role of p38 MAPK in astrocyte activation in a transient mouse MCAO model, Western blot was performed using protein isolated from ischemic cortex. We found that GFAP expression was increased in the ischemic cortex at day 4, and remained elevated up to day 10 after stroke, in parallel with a similar p38 MAPK activation pattern (Fig. 1A). Immunohistochemistry indicated that GFAP- and p38 MAPK- immune reactive cells were barely detectable in the ischemic core. However, these immune reactive cells were slightly increased 1 day (Fig. 1B), and dramatically increased 10 days after stroke in the peri-infarct area (Fig. 1B). These results indicated the potential involvement of p38 MAPK signaling in astrogliosis after ischemic stroke.

2.2. Inactivation of p38 MAPK inhibits astrocyte activation induced by transient OGD

We determined the effect of p38 inactivation in astrogliosis in primary astrocyte cultures using both pharmacological and genomic approaches. Our Western blot analysis indicated that OGD/reoxygenation insult induced astrogliosis evidenced by the increases of GFAP expression, which was associated with an activation of p38 MAPK (Fig. 2A). In addition, the increase of GFAP expression induced by transient OGD was totally blocked by the treatment of p38 inhibitor, SB239063 (Fig. 2A & B).

The involvement of p38 in astrogliosis was further evaluated using primary astrocyte cultures derived from conditional GFAP/p38 knockout mice. Western blot analysis of primary astrocyte cultures derived from wild type (WT) and GFAP/p38 knock out (GFAP/p38KO) demonstrated that knockout p38 MAPK dramatically decreased basal GFAP expression under normal cell culture condition (Fig 3A). Consistently, the transient OGD induced astrocyte activation in wild type astrocyte culture which was attenuated in p38 MAPK knockout astrocyte cultures (Fig 3B, C). Our gelatin zymography indicated that p38 MAPK knockout astrocytes had significant lower MMP-9 activity as compared with wild type astrocytes (Fig. 3D, E). We determined the expression of two important cytokines whose expression is regulated by p38 MAPK pathway. Results from quantitative PCR analysis indicated that conditional p38 knockout primary astrocyte cultures had significantly lower expression of the pro-inflammatory cytokine TNF-α (Fig 4A) and significantly higher expression of anti-inflammatory cytokine TGF-β (Fig 4B) when compared to wild type primary astrocyte cultures.

2.3. Inactivation of p38 MAPK attenuates scratch injury induced increase of GFAP expression

We investigated the role of p38 MAPK in scratch injury induced astrogliosis in primary astrocyte cultures. Our immunocytochemistry showed a robust increase in GFAP expression along the edge of the scratch in primary astrocyte cultures at 3 days after injury, which was

attenuated by the treatment of SB239063 (Fig. 5A). Similarly, wild type astrocytes showed a dramatic increase of GFAP expression and p38 MAPK activation after scratch, which was almost totally attenuated in primary astrocyte cultures derived from GFAP/p38 knock mice (Fig. 5B).

2.4. p38 MAPK inactivation attenuates astrocyte migration

We determined the role of p38 MAPK in astrocyte migration using *in vitro* wound healing assay. At 24 and 48 hrs after scratch injury large gaps were clearly evident in the SB239063 treated primary astrocyte culture as compared with wild type astrocyte cultures (Fig. 6A, B). Consistently, primary astrocyte cultures derived from p38 MAPK knockout mice have significant slower wound healing process when compared with wild type primary astrocyte cultures (Fig. 6C). In transwell migration assay, p38 MAPK inactivation by either SB239063 or p38 knockout significantly attenuates cell migration (Fig. 7A, B). To rule out the probability that the effect of p38 inactivation on wound healing and cell and migration assays is due to the potential action of p38 on cell proliferation, we determined the effect of p38 inhibition on growth curve and cell cycle in primary astrocyte cultures. No significant difference was observed in either primary astrocyte proliferation or cell cycle upon SB239063 treatment (Fig. 7C, D, and E).

2.5. Conditional GFAP/p38 knockout attenuates astrogliosis after ischemic stroke

In a pilot study, we chose transient MCAO model in which a lower mortality and smaller lesion was observed in GFAP/p38 knockout mice. To minimize the potential influence of infarct volume on astrogliosis, we determined the role of p38 MAPK in astrogliosis induced by ischemic stroke using a mouse permanent distal MCAO model. The mortality was 50% and 46% in littermates and GFAP/p38 knockout mice, respectively. The behavioral test battery indicated that there was no significant different in motor function recovery after ischemic stroke between GFAP/p38 knockout mice and littermate controls (Figure 8A, B, C, D). Cresyl violet staining of brain sections after permanent MCAO showed no significant difference in the size of the infarcts between GFAP/p38 knockout mice and wild type littermates (Figure 8E, F). Morphometric analysis of GFAP immunohistochemistry demonstrated that GFAP/p38 knockout mice had significantly less GFAP positive cells in the per-infarct region compared with the wild type littermates (Figure 9A). Further quantitative analysis of astrocyte size in the per-infarct area indicated that astrocytes were significantly fewer and smaller in GFAP/p38 knockout mice than wild type littermates ($p<0.001$) (Figure 9B, C). Western blot analysis indicated a significant reduction of GFAP expression in ischemic and non-ischemic cortex of GFAP/p38 knockout mice as compared with wild type ($p<0.05$) (Figure 9D & E).

3. Discussion

p38 MAPK has been well recognized as the key signaling in peripheral immune response. There is increasing evidence that p38 MAPK might also play a role in neuroinflammation in CNS. In primary neuron-glia co-cultures, activation of p38 MAPK has been found in both neuron and astrocyte following lipopolysaccharide treatment and inhibition of p38 partially blocked neuron death in the LPS-treated co-cultures (Xie et al., 2004). In an Alzheimer's

disease mouse model, p38 MAPK inhibitor has been shown to suppress brain proinflammatory cytokine up-regulation and attenuates synaptic dysfunction and behavioral deficits (Munoz et al., 2007). It has been suggested that p38 MAPK is involved in the cytokine-stimulated CCL2 and CCL7 production in primary astrocyte cultures (Thompson and Van Eldik, 2009). Activation of p38 MAPK has been reported to be involved in sciatic nerve ligation-induced proliferation of spinal cord astrocytes (Xu et al., 2007). Delayed induction of p38 MAPK in reactive astrocytes was found in mice brain after kainic acid-induced seizure (Che et al., 2001). In the present study, we provided both *in vitro* and *in vivo* evidence that p38 MAPK signaling pathway plays an important role in astrocyte activation and glial scar formation after ischemic stroke.

Clinically and experimentally, ischemic stroke is followed by inflammatory response contributing to both ischemic damage cascade and repairing process. Astrocytes in ischemic core and peri-infarct region undergo various responses to ischemic injury. In the mouse experimental ischemic stroke model, a dramatic loss of astrocyte in the ischemic core was observed evidenced by the loss of GFAP immune reactivity in the ischemic territory. In the peri-infarct region, a progressive astrogliosis was observed indicated by the increase of GFAP positive cells number and hypertrophy of GFAP positive cells. In addition, a similar pattern of change in p38 MAPK immunohistochemistry was found with a loss of p38 MAPK immune reactive cells in the ischemic core and increase of p38 MAPK immune reactive cells in the peri-infarct region. These findings suggest that p38 MAPK might be involved in the astrogliosis induced by ischemic stroke.

We determined the involvement of p38 MAPK in astrogliosis using primary astrocyte cultures. Inactivation of p38 MAPK was achieved by either a p38 inhibitor or using primary astrocyte derived from GFAP/p38 knockout mice. Our findings demonstrated that p38 MAPK signaling is involved in the astrocyte activation which could be attenuated by both pharmacological and genomic inactivation of p38 MAPK. p38 MAPK signaling pathway is also known to play a crucial role in synthesis and signaling of cytokines like TNF-α (Lee et al., 2000; Zarubin and Han, 2005) and TGF-β (Dziembowska et al., 2007) both of which are known to alter during reactive astrogliosis (Gao et al., 2013). Our study demonstrated that inactivation of p38 signaling significantly attenuated the proinflammatory cytokine TNF-α while at the same had a higher expression of anti-inflammatory cytokine TGF-β expression. Astrocyte migration in the CNS is a fundamental component of glial scarring (Auguste et al., 2007). There is an indication that p38 MAPK is involved in the cellular migration in epithelial wound healing process without affecting proliferation (Sharma et al., 2003). Our study suggested that inactivation of p38 MAPK attenuates astrocyte migration, evidenced by the wound healing and transwell migration assays. Matrix metalloproteinases (MMPs) degrade a variety of protein constituents in the extracellular matrix and thus remodel the peri-cellular microenvironment for astrocyte translocation and glial scar formation (Hsu et al., 2008). Consistently, our study demonstrated that inhibition of p38 MAPK decreases MMPs action in primary astrocyte culture. No effect of p38 inhibition on astrocyte proliferation and cell cycle was observed.

We determined the role of p38 in astrogliosis induced by ischemic stroke using mouse MCAO model. Since p38 inhibition has been found to be protective in ischemic stroke

model (Barone et al., 2001; Legos et al., 2002; Nito et al., 2008; Nozaki et al., 2001; Piao et al., 2003; Strassburger et al., 2008), conditional GFAP/p38 knockout may provide protective effect in the transient MCAO model. To minimize the potential influences of infarct size in astrogliosis, we adopted a permanent distal MCAO model to ensure similar extent ischemic lesion size in both conditional GFAP/p38 knockout mice and littermates. Similar mortality and motor function outcome were observed in GFAP/p38 knockout mice and littermate controls. No significant difference in the infarct volume was found between GFAP/p38 knockout and wild mice. We predict that the intense and permanent ischemic insult might have dampened the potential beneficial effect of astrocyte specific p38 deletion. Our unbiased stereological analysis of GFAP immunohistochemistry indicated conditional knockout of p38 in astrocyte significantly attenuated astrogliosis at the early stage after ischemic stroke.

Compelling evidence has indicated that reactive astrogliosis is a complex process either through loss of essential functions performed by astrocytes or by gain of detrimental effects after activation (Sofroniew, 2009). It has been long recognized that astrogliosis may have a pathological effect by interfering with the function of residual neuronal circuits. Many studies have demonstrated the detrimental effects of glial scar on axonal regeneration after ischemic injury (Cua et al., 2013; Hill et al., 2012; Iseki et al., 2012), preventing axonal remyelination and inhibiting axonal regeneration (Sofroniew, 2009; Wang and Shuaib, 2002). The inhibitory action of glial scar on axonal regeneration may impair motor function recovery. On the other hand, increasing evidence has indicated that reactive astrocytes have potentially beneficial effect. Cell type-specific and temporal control of astrocyte deletion has been applied in combination with various forms of experimental CNS insults, including forebrain stab injury (Bush et al., 1999), spinal cord injury (Faulkner et al., 2004), traumatic brain injury (Myer et al., 2006) and autoimmune encephalomyelitis (EAE) (Voskuhl et al., 2009). In all of these models, ablation of proliferating reactive astrocytes disrupted scar formation, which in turn resulted in increased spread and persistence of inflammatory cells, failure of BBB repairing, increased tissue damage and lesion size, increased neuronal loss and demyelination, and exacerbation of clinical signs or impaired function recovery, providing evidence that scar forming astrocytes play essential roles in neural protection and repair (Sofroniew, 2009).

Knockout of molecules produced by reactive astrocytes has provided insight regarding the roles of specific molecules in reactive astrogliosis (Correa-Cerro and Mandell, 2007; Sofroniew, 2009). Double deletion of GFAP and vimentin reduces astrogliosis and increases axon regeneration, but exacerbates ischemic stroke (Li et al., 2008) by increasing lesion size and worsening outcome. In contrast, conditional deletion or functional knockdown in astrocytes of the signaling molecules suppressor of cytokine signaling or NFκB reduces inflammation and lesion size after spinal cord injury or EAE (Brambilla et al., 2009; Okada et al., 2006). Taken together, these findings indicate complex functions of reactive astrogliosis, which might differ in response to different signaling mechanisms in a context-specific manner (Sofroniew, 2009). Thus, intervention of specific signaling pathway might be able to augment or block specific function of reactive astrocyte, hence, enhance neural repair process without comprising the beneficial effect of astrogliosis. Our study indicated that p38 signaling is involved in astrogliosis after ischemic stroke and that inactivation of

p38 MAPK attenuates astrogliosis without affecting the acute outcome in a permanent MCAO model. As stroke induced neurogenesis and axonal sprouting in the peri-infarct area matures in a much delayed manner (Kuge et al., 2009; Li and Carmichael, 2006), future studies are needed to examine the effect of p38 signaling inactivation on neurogenesis, axonal sprouting, and long term functional recovery in experimental ischemic stroke models. In addition, astrocyte has been shown to play a critical role in angiogenesis after ischemic stroke (Hayakawa et al., 2010). Inhibition of p38 signaling might affect the angiogenesis process induced by ischemic stroke through its action on astrogliosis.

In our current study, the role of p38 in reactive astrogliosis was determined in primary astrocyte cultures in order to determine the fundamental mechanism underlying astrocyte activation in response to ischemic injury which is very difficult *in vivo* considering the interaction of multiple cell types and the expression of p38MAPK in both neuron and glial cells. Our *in vitro* studies employed hypoxia-reoxygenation model to simulate ischemic stroke. Scratch injury assay, a most commonly used model of *in vitro* astrogliosis (Etienne-Manneville, 2006; Parmentier-Batteur et al., 2011; Zhu et al., 2007) was used as an additional model of cellular injury to further validate our findings from hypoxia-reoxygenation model. However as with *in vitro* models our study presented certain limitations such as short duration of endpoints compared to *in vivo* studies. In addition, our current in vivo study used constitutive astrocyte specific p38 knockout mouse model which does not enable to study the role of p38 in astrogliosis in a temporal dependent manner. Further studies using inducible astrocyte specific p38 MAPK knockout mouse model may provide critical insight for the action of spatiotemporal p38 inhibition on glial scar formation and functional outcome after ischemic stroke.

In summary, the present study provides the first in vitro and in vivo evidence that p38 MAPK signaling pathway plays an important role in the astrogliosis after ischemic stroke. The neuroprotective effect of acute p38 MAPK inhibition against ischemic stroke has been well defined in experimental ischemic stroke models (Barone et al., 2001; Legos et al., 2002; Nito et al., 2008; Nozaki et al., 2001; Piao et al., 2003; Strassburger et al., 2008). The robust neuroprotection induced by p38 MAPK inhibition emphasizes a significant opportunity for targeting p38 MAPK for the treatment of ischemic stroke. However, the translational potential of p38 inhibition to clinical practice for acute stroke treatment is very limited, given the short therapeutic window of neuroprotective intervention for acute stroke treatment and the disappointing outcome of the neuroprotection clinical trials. On the other hand, given the progressive course of astrogliosis and well-established inhibitory action of glial scar on axonal sprouting and neurite growth, p38 MAPK may serve as an essential target for dissecting the molecular mechanism underlying glial scar formation after ischemic stroke. In addition, given that some p38 MAPK inhibitors are already in clinical trials, p38 inhibition may provide a novel therapy for temporal control of glial scar formation, hence, enhance axonal sprouting and neurite growth and improve stroke recovery.

4. Materials and Methods

4.1. Animals

Animal experimentation was approved by Institutional Animal Care and Use Committee (IACUC) of University of North Texas Health Science Center. Adult male C57B/6 mice (3 months old: Charles River, Wilmington, MA) were used for the study. The astrocyte specific p38 knockout mice were established by crossing two mouse lines, the *FloxP* p38α and Tg (GFAP-cre) 25MEs (JAX laboratory). Flox p38α has floxed alleles that were generated by homologous recombination in embryonic stem cells (Lexicon), in which the first exon (containing ATG) was flanked by two loxP sites (Engel et al., 2005). When crossed with *FloxP p38α mice*, GFAP-cre mediated recombination results in astrocyte-specific deletion of the p38α. In our breeding strategy, Flox $p38^{+/+}$ were cross bred with ($Flox^{-}p38^{+/+}$) / ($GFAP^{-}cre^{+/-}$ mice), which generate 50% conditional astrocyte p38 knockout mice and 50% wide type littermates.

4.2 Genotyping

All the pups were weaned at age of 4 weeks and ID chips were implanted. Tails were cut and lysed overnight at 55 °C. The lysate was centrifuged at 10,000 rpm for 10 min and supernatant was collected. The supernatant was diluted at 1:100 and used for PCR using standard Cre and p38 primers: GFAP CreF, 5'-AGCGATCGCTGCCAGGAT-3'; GFAP CreR, 5'-ACCAGCGTTTTCGTTCTGCC-3'; p38 B12-125L, 5'-AGTCCCCGAGAGTTCCTGCCTC-3'; p38 B12-41L, 5'-TCCTACGAGCGTCGGCAAGGT-3' (Engel et al., 2005). Thirty-five PCR cycles were run consisting of denaturation at 95 °C for 1 min, annealing at 60 °C for 2 min, and extension at 72 °C for 1 min, followed by a final extension for 5 min. The PCR products were resolved on a 2.0% agarose gel. The transgenic GFAP cre/ Flox p38 mice were then confirmed by the presence of transgene at 190 base pair (internal positive control at 700 bp).

4.3. Middle cerebral artery occlusion models

All surgeries were conducted under 2.0% isoflurane anesthesia. Body temperature was maintained at 37 ± 0.5 °C with a thermostat-controlled heating blanket during the entire procedure. Transient MCAO was performed to induce transient focal cerebral ischemia in adult C57B/6 mice. A midline incision was made on the neck. Common carotid artery, external carotid artery and internal carotid artery (ICA) were dissected from the connective tissue. A silicon coated 6-0 nylon monofilament was inserted into the left ICA and advanced till it occluded the origin of MCA. The MCA was occluded for 90 minutes and then reperfusion was obtained by withdrawing the suture. The animals were sacrificed at days 1, 4 and 10 after MCAO and brains were harvested for immunohistochemistry and Western blot analysis. In a separate set of mice (11 to 12 months of age), permanent distal MCAO was induced in GFAP/p38 knockout mice (n=15) and wild type littermates (n=8) via craniectomy as previously described (Jin, 2010 #32). A skin incision was made between the left eye and ear. A burr hole was drilled through the temporal bone. The dura mater was removed and the MCA was occluded permanently using a bipolar coagulator. The mice were sacrificed at 4 days after stroke and brain harvested for immunohistochemistry and Western blot analysis.

4.4. Primary astrocyte cultures

Primary astrocyte cultures were prepared from 1-day old pups of C57B6 mice, conditional GFAP/p38 MAPK knockout mice, or wild type littermates. Under aseptic conditions cerebral cortices were dissected and placed in sterile phenol red free Dulbecco's Modified Eagle's Medium (DMEM, 4500 mg/l Glucose, 4 mM L-Glutamine, 1 mM Sodium Pyruvate, Thermo Scientific) containing 1% of streptomycin (10,000 μg/ml)-penicillin (10,000 units/ml). Cerebral cortices were then incubated in 0.5% trypsin at 37°C for 20 minutes and using a sterile glass Pasteur pipette were dissociated into a single cell suspension. Primary astrocytes were then cultured in High Glucose DMEM (4500 mg/L Glucose, 4 mM L-Glutamine, 1 mM Sodium Pyruvate, Thermo Scientific) containing 10% FBS and 1% of streptomycin (10,000 μg/ml)-penicillin (10,000 units/ml) in a humidified incubator at 37 °C and 5% CO_2. At 90% confluency the microglia in the cultures was removed by shaking constantly for 48 hrs. Primary astrocytes isolated from GFAP/p38 knockout mice and littermates were further confirmed by Western blot of p38. For p38 MAPK inhibition, cells were treated with SB239063 diluted in the media at a final concentration of 10 μg/ml.

4.5. In vitro hypoxia-reoxygenation model

Astrocytes were seeded in 6-well culture plates at a density of 2.5×10^5 cells/well in high glucose DMEM (4500 mg/L Glucose, 4 mM L-Glutamine, 1 mM Sodium Pyruvate) with 10% FBS and 1% of streptomycin (10,000 μg/ml)-penicillin (10,000 units/ml). When the cells reached 80% confluence, media was removed and cells were washed twice with sterile PBS and replaced with glucose, pyruvate and FBS free DMEM. The cell culture plates were then placed in anaerobic chamber containing 0.5% O_2 and 5% CO_2 for 3 hrs. At the end of oxygen glucose deprivation (OGD) the cells were replenished with FBS free DMEM containing D-glucose (4500 mg/L) and pyruvate (1 mM) and were placed in incubator for 24 hrs. For inhibitor studies the cells were pre-treated with p38 MAPK inhibitor, SB239063 (10 μg/ml), 2 hrs before OGD.

4.6. Wound healing assay

The astrocytes (2.5×10^5 cells/well) were cultured in high glucose DMEM (10% FBS and 1% of streptomycin (10,000 μg/ml)-penicillin (10,000 units/ml)) to a monoconfluent layer in 6-well cell culture plates. Using sterile 200 μl pipette tip scratches were made on the cell layer, the plates were then rinsed with sterile PBS to remove cell debris and replaced with fresh cell culture media or SB239063 (10 μg/ml) containing media. At 0, 24 and 48 hrs after scratch, cells were stained with Calcein AM (10 μM), fluorescent images were obtained randomly using a Zeiss fluorescence microscope. For quantitative analysis, images from Calcein AM staining were used. Using NIH Image J software the distance between the two edges of the scratch was determined and these values were used to quantify and plot wound healing.

4.7. Migration assay

Migration assay was performed with BD matrigel™ invasion chamber (24 well) according to manufacturer's instruction. Briefly, the transwell inserts were rehydrated in FBS free DMEM for 2 hrs at 37°C. After rehydration a suspension 1×10^5 cells/ml in FBS free

DMEM was added to each insert and 5% FBS as chemoattractant to bottom wells and were incubated for 22 hrs. At the end incubation period the insert were removed from the transwell and non migrating cells were removed by gently swiping the interior of the transwell using a cotton swab. The migrating cells were then fixed with methanol (100%) and stained with Toluidine Blue (1% in Borax solution). The inserts were air-dried and images of the migrated cells were taken using a Zeiss Microscope. For quantitative analysis, the number of cells migrated in each insert was counted from the images and then plotted using Prism software. For p38MAPK inhibition study, SB239063 was added to both cell suspension and chemoattractant media.

4.8. Growth curve assay and cell cycle analysis

For growth curve assay, primary astrocytes were seeded into 12-well culture plates at 200,000 cells/well in 0.5 ml of DMEM with pyruvate (10% FBS and 1% of streptomycin (10,000 μg/ml)-penicillin (10,000 units/ml)). Drugs were added to each well to obtain the desired concentration in a final volume of 1 ml per well. Day of seeding was considered day 0. Plates were incubated in a humidified incubator at 37 °C and 5% CO_2. Cells were harvested on each indicated day using 0.25% Trypsin-EDTA (Gibco) and counted using an inverted phase contrast Zeiss microscope. For cell cycle analysis, Cells were plated at a density of 200,000 cells/well and attached overnight. The following day, the cells were deprived of FBS overnight to standardize the cell cycle followed by fresh DMEM containing 10% FBS and the indicated concentration of drug. At the indicated times, cells were harvested using 0.5% trypsin (Invitrogen) and washed with Wash Buffer (0.1% FBS in PBS) twice. Cells were fixed in ice cold 70% ethanol for 45 minutes at 4 °C. Ethanol was removed by washing twice with PBS, the cells were then incubated with propidium iodide (PI) (40 μg/ml) and RNAse (10 μg/ml) for 30 min at 37 °C. Samples were analyzed using Beckman Coulter FC500 Flow Cytometry Analyzer.

4.9. Immunohistochemistry and immunocytochemistry

For immunohistochemistry, the animals were anesthetized with isoflurane, decapitated and transcardially perfused with ice cold normal saline and 4% formalin. The brains were removed and fixed in 4% formalin and further processed to be embedded in paraffin. Using a microtome 10 micron thick sections were prepared. Sections were stained with primary antibodies for GFAP (Santa Cruz, 1:100), p38 (Cell signaling, 1:100), Phoshporylated p38 (Cell signaling, 1:100) followed by secondary poly horse radish peroxidase (HRP) and 3,3'-Diaminobenzidine (DAB) staining. For immunocytochemistry, primary astrocytes were cultured on a glass cover slip in DMEM containing 10% FBS and 1% Streptomycin (10,000 μg/ml)-Penicillin (10,000 units/ml). Astrocytes monolayer was fixed in 4% formalin for 10 minutes and permeabilized with 1% Triton-X for 15 minutes at room temperature. After blocking with goat serum (5%) for 30 minutes, primary antibodies for GFAP (Santa Cruz, 1:100) or phoshphorylated p38 (Cell signaling, 1:100) were applied and incubated overnight at 4 °C followed by species specific secondary antibodies. Images were taken using a Zeiss Microscope (Carl Zeiss).

4.10. Gelatin Zymography

Gelatinolytic activity of Matrix Metalloproteases (MMP 2 & 9) in the media was determined by zymography. At the end of reoxygenation, media from the cultures was collected and samples were resolved on 8% SDS-Polyacrylamide gels containing 0.1% gelatin under non-reducing condition. After electrophoresis, gels were washed in a wash buffer containing (2.5% Triton-x, 7.45 mM, CaCl2, 1 μM ZnCl2, 50mM Tris-HCl, pH 7.4) at 37 °C for 24 hrs. The gels were then stained with Commassie blue (0.25% Commassie Blue, 45% methanol, 10% acetic acid) for 2 hrs and destained with a destaining solution (10% acetic acid and 30% methanol) for 3 hrs. Using Biospectrum 500 UVP imaging system densitometry analysis was performed on the zymographs to quantify the gelatinolytic activity of the MMPs.

4.11. Western blots analysis

Cell and brain protein samples were prepared in lysis buffer containing protease and phosphatase inhibitors. To ensure equal loading, protein concentration was determined using Pierce 660nm Protein assay reagent (Thermo Scientific). Proteins were then resolved on 10% gel and transferred to a nitrocellulose membrane. After blocking with 5% milk, blots were incubated overnight with primary antibodies against GFAP (Santa Cruz, 1:500), p38 (Cell signaling, 1:500), phoshphorylated p38 (Cell signaling, 1:1000) or actin (Santa Cruz, 1:1000) at 4 °C followed by secondary antibody (Goat, Jackson Immunoresearch, West Grove, PA). Chemiluminescence signal was detected with Biospectrum500 UVP imaging system. Protein band density of GFAP, p38, Pp38 and actin was then determined and quantified using the densitometry analysis. All the protein band density values were normalized to their respective actin band density and were plotted using Prism, statistical software.

4.12. Quantitative real-time PCR

RNAs from wild type and conditional p38 knockout astrocytes were extracted using Trizol LS Reagent according to manufacturer's instruction. Quantitative real-time PCR was performed using SYBR Green PCR Master Mix (Promega) and 7300 Real-Time PCR System from Applied Biosystems. Two-step real-time PCR protocol was used (95 °C for 15 sec, 60 °C for 60 sec extension and detection, 40 cycles). Sequences of primers for real-time PCR are listed as following:

TNFα: Forward 5′GCCTCTTCTCATTCCTGCTTGT 3′

Reverse 5′ CAGGCTTGTCACTCGAATTTTG 3′

TGFβ: Forward 5′ TTGCTTCAGCTCCACAGAGAAG 3′

Reverse 5′ CCAGACAGAAGTTGGCATGGTA 3′

4.13. Behavioral test

For walk initiation, the mice were placed in a circle of diameter of 10 cm (approximately one animal length) on an open table and the latency for the animal to walk out of the circle was recorded. For negative geotaxis, the latency of the animals to turn (90°) and reverse (180°) when placed on an inclined (45°) flat surface was measured. Latencies during walk

initiation and negative geotaxis were recorded immediately before surgery and on days 1 and 4 after surgery. Ladder rung walking test was used to assess and quantify motor dysfunction after MCAO as previously described (Metz and Whishaw, 2002). Briefly, the animals were made to walk on an apparatus 122 cm long with horizontal plastic rungs placed 7 mm apart. All the animals underwent 3 testing trials prior to surgery and after surgery on day 1 and day 4. During each trail all the foot faults and stepping errors for both forelimb and hind limb were recorded for each animal. At the end of the study means of 3 trials were calculated and values were used to plot the foot fault using Prism statistical soft ware.

4.14. Quantification of infarct volume

The brains were removed and fixed in 4% formalin. 10 μm thick paraffin embedded sections were prepared and stained with 1% cresyl violet to define non-infarct tissue. Using the NIH Image program the area of the non-ischemic (contralateral) hemisphere (A), non-infarct area of the ischemic hemisphere (B), and total brain was measured in each section. Infarct volume was expressed as a percentage of the area of the contralateral hemisphere (= (A−B)/A*100) and multiplied with distance between sections, as previously described (Jin et al., 2010).

4.15. Astrogliosis morphometric analysis

Serial microscopic images were taken in the border area of the ischemic lesion for unbiased stereological analysis of astrogliosis induced by ischemic stroke. Six sampling frames (40× objective field) were randomly selected per section in layer II-III of the cortex within 400 μm from the border of the infarction (Barreto et al., 2011). For analysis and quantification both cell number and sizes of GFAP immunoreactive cells were measured using the nucleator method. According to this method only those cells with defined nuclear outline were counted and those cells without any defined nuclear outline were not included in cell counts (Herrmann et al., 2008). To eliminate bias in quantitative analysis, all the images were assigned a code consisting of a random alphabet and a numeric, and thus, the individual doing cell counts is blinded for the region of the brain (ischemic vs. non-ischemic hemisphere) and genotype of the transgenic mice (wild type vs. GFAP/p38 knockout). At the end of analysis the cell counts were matched to their respective region and groups. For cell size analysis, Adobe Photoshop CS6 image software was used to create a binary image with 600 pixels/inch resolution. Then using ROI manager tool of NIH Image J software the area of each cell was determined at constant threshold for all the images. All the cell sizes were then pooled in each group and plotted as % of wild type cell area using Prism statistical software.

4.16. Statistical analysis

Graph Pad Prism 5 was used for statistical analysis. All the results are expressed as mean ± standard error of mean (SEM). When comparing two groups a t-test was used to identify any significant differences. For comparison of multiple groups, two-way analysis of variance was used and post-hoc Bonferroni analysis was done to identify the significant differences. $p < 0.05$ was considered as statistically significant.

Acknowledgments

This work was partly supported by National Institutes of Health grants R01NS054687, R01NS054651, National Natural Science Foundation of China Grant 81228009, and ECP was a predoctoral trainee supported by T32 AG020494.

References

Auguste KI, Jin S, Uchida K, Yan D, Manley GT, Papadopoulos MC, Verkman AS. Greatly impaired migration of implanted aquaporin-4-deficient astroglial cells in mouse brain toward a site of injury. Faseb J. 2007; 21:108–116. [PubMed: 17135365]

Barone FC, Irving EA, Ray AM, Lee JC, Kassis S, Kumar S, Badger AM, Legos JJ, Erhardt JA, Ohlstein EH, Hunter AJ, Harrison DC, Philpott K, Smith BR, Adams JL, Parsons AA. Inhibition of p38 mitogen-activated protein kinase provides neuroprotection in cerebral focal ischemia. Med Res Rev. 2001; 21:129–145. [PubMed: 11223862]

Barreto GE, Sun X, Xu L, Giffard RG. Astrocyte proliferation following stroke in the mouse depends on distance from the infarct. PLoS One. 2011; 6:e27881. [PubMed: 22132159]

Brambilla R, Bracchi-Ricard V, Hu WH, Frydel B, Bramwell A, Karmally S, Green EJ, Bethea JR. Inhibition of astroglial nuclear factor kappaB reduces inflammation and improves functional recovery after spinal cord injury. J Exp Med. 2005; 202:145–156. [PubMed: 15998793]

Brambilla R, Persaud T, Hu X, Karmally S, Shestopalov VI, Dvoriantchikova G, Ivanov D, Nathanson L, Barnum SR, Bethea JR. Transgenic inhibition of astroglial NF-kappa B improves functional outcome in experimental autoimmune encephalomyelitis by suppressing chronic central nervous system inflammation. J Immunol. 2009; 182:2628–2640. [PubMed: 19234157]

Bush TG, Puvanachandra N, Horner CH, Polito A, Ostenfeld T, Svendsen CN, Mucke L, Johnson MH, Sofroniew MV. Leukocyte infiltration, neuronal degeneration, and neurite outgrowth after ablation of scar-forming, reactive astrocytes in adult transgenic mice. Neuron. 1999; 23:297–308. [PubMed: 10399936]

Che Y, Yu YM, Han PL, Lee JK. Delayed induction of p38 MAPKs in reactive astrocytes in the brain of mice after KA-induced seizure. Brain Res Mol Brain Res. 2001; 94:157–165. [PubMed: 11597776]

Codeluppi S, Svensson CI, Hefferan MP, Valencia F, Silldorff MD, Oshiro M, Marsala M, Pasquale EB. The Rheb-mTOR pathway is upregulated in reactive astrocytes of the injured spinal cord. J Neurosci. 2009; 29:1093–1104. [PubMed: 19176818]

Correa-Cerro LS, Mandell JW. Molecular mechanisms of astrogliosis: new approaches with mouse genetics. J Neuropathol Exp Neurol. 2007; 66:169–176. [PubMed: 17356378]

Cua RC, Lau LW, Keough MB, Midha R, Apte SS, Yong VW. Overcoming neurite-inhibitory chondroitin sulfate proteoglycans in the astrocyte matrix. Glia. 2013; 61:972–984. [PubMed: 23554135]

Dziembowska M, Danilkiewicz M, Wesolowska A, Zupanska A, Chouaib S, Kaminska B. Cross-talk between Smad and p38 MAPK signalling in transforming growth factor beta signal transduction in human glioblastoma cells. Biochem Biophys Res Commun. 2007; 354:1101–1106. [PubMed: 17276399]

Engel FB, Schebesta M, Duong MT, Lu G, Ren S, Madwed JB, Jiang H, Wang Y, Keating MT. p38 MAP kinase inhibition enables proliferation of adult mammalian cardiomyocytes. Genes Dev. 2005; 19:1175–1187. [PubMed: 15870258]

Etienne-Manneville S. In vitro assay of primary astrocyte migration as a tool to study Rho GTPase function in cell polarization. Methods Enzymol. 2006; 406:565–578. [PubMed: 16472688]

Faulkner JR, Herrmann JE, Woo MJ, Tansey KE, Doan NB, Sofroniew MV. Reactive astrocytes protect tissue and preserve function after spinal cord injury. J Neurosci. 2004; 24:2143–2155. [PubMed: 14999065]

Ferrer I, Friguls B, Dalfo E, Planas AM. Early modifications in the expression of mitogen-activated protein kinase (MAPK/ERK), stress-activated kinases SAPK/JNK and p38, and their phosphorylated substrates following focal cerebral ischemia. Acta Neuropathol. 2003; 105:425–437. [PubMed: 12677442]

Gao Z, Zhu Q, Zhang Y, Zhao Y, Cai L, Shields CB, Cai J. Reciprocal modulation between microglia and astrocyte in reactive gliosis following the CNS injury. Mol Neurobiol. 2013; 48:690–701. [PubMed: 23613214]

Hayakawa K, Nakano T, Irie K, Higuchi S, Fujioka M, Orito K, Iwasaki K, Jin G, Lo EH, Mishima K, Fujiwara M. Inhibition of reactive astrocytes with fluorocitrate retards neurovascular remodeling and recovery after focal cerebral ischemia in mice. J Cereb Blood Flow Metab. 2010; 30:871–882. [PubMed: 19997116]

Herrmann JE, Imura T, Song B, Qi J, Ao Y, Nguyen TK, Korsak RA, Takeda K, Akira S, Sofroniew MV. STAT3 is a critical regulator of astrogliosis and scar formation after spinal cord injury. J Neurosci. 2008; 28:7231–7243. [PubMed: 18614693]

Hill JJ, Jin K, Mao XO, Xie L, Greenberg DA. Intracerebral chondroitinase ABC and heparan sulfate proteoglycan glypican improve outcome from chronic stroke in rats. Proc Natl Acad Sci U S A. 2012; 109:9155–9160. [PubMed: 22615373]

Hsu JY, Bourguignon LY, Adams CM, Peyrollier K, Zhang H, Fandel T, Cun CL, Werb Z, Noble-Haeusslein LJ. Matrix metalloproteinase-9 facilitates glial scar formation in the injured spinal cord. J Neurosci. 2008; 28:13467–13477. [PubMed: 19074020]

Iseki K, Hagino S, Nikaido T, Zhang Y, Mori T, Yokoya S, Hozumi Y, Goto K, Wanaka A, Tase C. Gliosis-specific transcription factor OASIS coincides with proteoglycan core protein genes in the glial scar and inhibits neurite outgrowth. Biomed Res. 2012; 33:345–353. [PubMed: 23268958]

Jin K, Mao X, Xie L, Greenberg RB, Peng B, Moore A, Greenberg MB, Greenberg DA. Delayed transplantation of human neural precursor cells improves outcome from focal cerebral ischemia in aged rats. Aging Cell. 2010; 9:1076–1083. [PubMed: 20883527]

Krupinski J, Slevin M, Marti E, Catena E, Rubio F, Gaffney J. Time-course phosphorylation of the mitogen activated protein (MAP) kinase group of signalling proteins and related molecules following middle cerebral artery occlusion (MCAO) in rats. Neuropathol Appl Neurobiol. 2003; 29:144–158. [PubMed: 12662322]

Kuge A, Takemura S, Kokubo Y, Sato S, Goto K, Kayama T. Temporal profile of neurogenesis in the subventricular zone, dentate gyrus and cerebral cortex following transient focal cerebral ischemia. Neurol Res. 2009; 31:969–976. [PubMed: 19138475]

Kumar S, Boehm J, Lee JC. p38 MAP kinases: key signalling molecules as therapeutic targets for inflammatory diseases. Nat Rev Drug Discov. 2003; 2:717–726. [PubMed: 12951578]

Lee YB, Schrader JW, Kim SU. p38 map kinase regulates TNF-alpha production in human astrocytes and microglia by multiple mechanisms. Cytokine. 2000; 12:874–880. [PubMed: 10880231]

Legos JJ, Erhardt JA, White RF, Lenhard SC, Chandra S, Parsons AA, Tuma RF, Barone FC. SB 239063, a novel p38 inhibitor, attenuates early neuronal injury following ischemia. Brain Res. 2001; 892:70–77. [PubMed: 11172750]

Legos JJ, McLaughlin B, Skaper SD, Strijbos PJ, Parsons AA, Aizenman E, Herin GA, Barone FC, Erhardt JA. The selective p38 inhibitor SB-239063 protects primary neurons from mild to moderate excitotoxic injury. Eur J Pharmacol. 2002; 447:37–42. [PubMed: 12106800]

Li L, Lundkvist A, Andersson D, Wilhelmsson U, Nagai N, Pardo AC, Nodin C, Stahlberg A, Aprico K, Larsson K, Yabe T, Moons L, Fotheringham A, Davies I, Carmeliet P, Schwartz JP, Pekna M, Kubista M, Blomstrand F, Maragakis N, Nilsson M, Pekny M. Protective role of reactive astrocytes in brain ischemia. J Cereb Blood Flow Metab. 2008; 28:468–481. [PubMed: 17726492]

Li S, Carmichael ST. Growth-associated gene and protein expression in the region of axonal sprouting in the aged brain after stroke. Neurobiol Dis. 2006; 23:362–373. [PubMed: 16782355]

Metz GA, Whishaw IQ. Cortical and subcortical lesions impair skilled walking in the ladder rung walking test: a new task to evaluate fore- and hindlimb stepping, placing, and co-ordination. J Neurosci Methods. 2002; 115:169–179. [PubMed: 11992668]

Munoz L, Ralay Ranaivo H, Roy SM, Hu W, Craft JM, McNamara LK, Chico LW, Van Eldik LJ, Watterson DM. A novel p38 alpha MAPK inhibitor suppresses brain proinflammatory cytokine up-regulation and attenuates synaptic dysfunction and behavioral deficits in an Alzheimer's disease mouse model. J Neuroinflammation. 2007; 4:21. [PubMed: 17784957]

Myer DJ, Gurkoff GG, Lee SM, Hovda DA, Sofroniew MV. Essential protective roles of reactive astrocytes in traumatic brain injury. Brain. 2006; 129:2761–2772. [PubMed: 16825202]

Nito C, Kamada H, Endo H, Niizuma K, Myer DJ, Chan PH. Role of the p38 mitogen-activated protein kinase/cytosolic phospholipase A2 signaling pathway in blood-brain barrier disruption after focal cerebral ischemia and reperfusion. J Cereb Blood Flow Metab. 2008; 28:1686–1696. [PubMed: 18545259]

Nozaki K, Nishimura M, Hashimoto N. Mitogen-activated protein kinases and cerebral ischemia. Mol Neurobiol. 2001; 23:1–19. [PubMed: 11642541]

Okada S, Nakamura M, Katoh H, Miyao T, Shimazaki T, Ishii K, Yamane J, Yoshimura A, Iwamoto Y, Toyama Y, Okano H. Conditional ablation of Stat3 or Socs3 discloses a dual role for reactive astrocytes after spinal cord injury. Nat Med. 2006; 12:829–834. [PubMed: 16783372]

Parmentier-Batteur S, Finger EN, Krishnan R, Rajapakse HA, Sanders JM, Kandpal G, Zhu H, Moore KP, Regan CP, Sharma S, Hess JF, Williams TM, Reynolds IJ, Vacca JP, Mark RJ, Nantermet PG. Attenuation of scratch-induced reactive astrogliosis by novel EphA4 kinase inhibitors. J Neurochem. 2011; 118:1016–1031. [PubMed: 21736568]

Piao CS, Che Y, Han PL, Lee JK. Delayed and differential induction of p38 MAPK isoforms in microglia and astrocytes in the brain after transient global ischemia. Brain Res Mol Brain Res. 2002; 107:137–144. [PubMed: 12425942]

Piao CS, Kim JB, Han PL, Lee JK. Administration of the p38 MAPK inhibitor SB203580 affords brain protection with a wide therapeutic window against focal ischemic insult. J Neurosci Res. 2003; 73:537–544. [PubMed: 12898538]

Ransohoff RM, Brown MA. Innate immunity in the central nervous system. J Clin Invest. 2012; 122:1164–1171. [PubMed: 22466658]

Sharma GD, He J, Bazan HE. p38 and ERK1/2 coordinate cellular migration and proliferation in epithelial wound healing: evidence of cross-talk activation between MAP kinase cascades. J Biol Chem. 2003; 278:21989–21997. [PubMed: 12663671]

Sofroniew MV. Molecular dissection of reactive astrogliosis and glial scar formation. Trends Neurosci. 2009; 32:638–647. [PubMed: 19782411]

Strassburger M, Braun H, Reymann KG. Anti-inflammatory treatment with the p38 mitogen-activated protein kinase inhibitor SB239063 is neuroprotective, decreases the number of activated microglia and facilitates neurogenesis in oxygen-glucose-deprived hippocampal slice cultures. Eur J Pharmacol. 2008; 592:55–61. [PubMed: 18638472]

Takeda K, Ichijo H. Neuronal p38 MAPK signalling: an emerging regulator of cell fate and function in the nervous system. Genes Cells. 2002; 7:1099–1111. [PubMed: 12390245]

Thompson WL, Van Eldik LJ. Inflammatory cytokines stimulate the chemokines CCL2/MCP-1 and CCL7/MCP-3 through NFkB and MAPK dependent pathways in rat astrocytes [corrected]. Brain Res. 2009; 1287:47–57. [PubMed: 19577550]

Voskuhl RR, Peterson RS, Song B, Ao Y, Morales LB, Tiwari-Woodruff S, Sofroniew MV. Reactive astrocytes form scar-like perivascular barriers to leukocytes during adaptive immune inflammation of the CNS. J Neurosci. 2009; 29:11511–11522. [PubMed: 19759299]

Wang CX, Shuaib A. Involvement of inflammatory cytokines in central nervous system injury. Prog Neurobiol. 2002; 67:161–172. [PubMed: 12126659]

Xie Z, Smith CJ, Van Eldik LJ. Activated glia induce neuron death via MAP kinase signaling pathways involving JNK and p38. Glia. 2004; 45:170–179. [PubMed: 14730710]

Xu M, Bruchas MR, Ippolito DL, Gendron L, Chavkin C. Sciatic nerve ligation-induced proliferation of spinal cord astrocytes is mediated by kappa opioid activation of p38 mitogen-activated protein kinase. J Neurosci. 2007; 27:2570–2581. [PubMed: 17344394]

Zarubin T, Han J. Activation and signaling of the p38 MAP kinase pathway. Cell Res. 2005; 15:11–18. [PubMed: 15686620]

Zhu Z, Zhang Q, Yu Z, Zhang L, Tian D, Zhu S, Bu B, Xie M, Wang W. Inhibiting cell cycle progression reduces reactive astrogliosis initiated by scratch injury in vitro and by cerebral ischemia in vivo. Glia. 2007; 55:546–558. [PubMed: 17243097]

Highlights

1. We established a novel **conditional astrocyte specific p38MAPK knockout** mouse model.
2. We determined the role of p38MAPK in reactive astrogliosis both *in vitro* and *in vivo*.
3. Inactivation of p38 MAPK attenuated reactive astrogliosis *in vitro*.
4. Conditional astrocyte specific p38 knockout attenuated astrogliosis induced by MCAO.

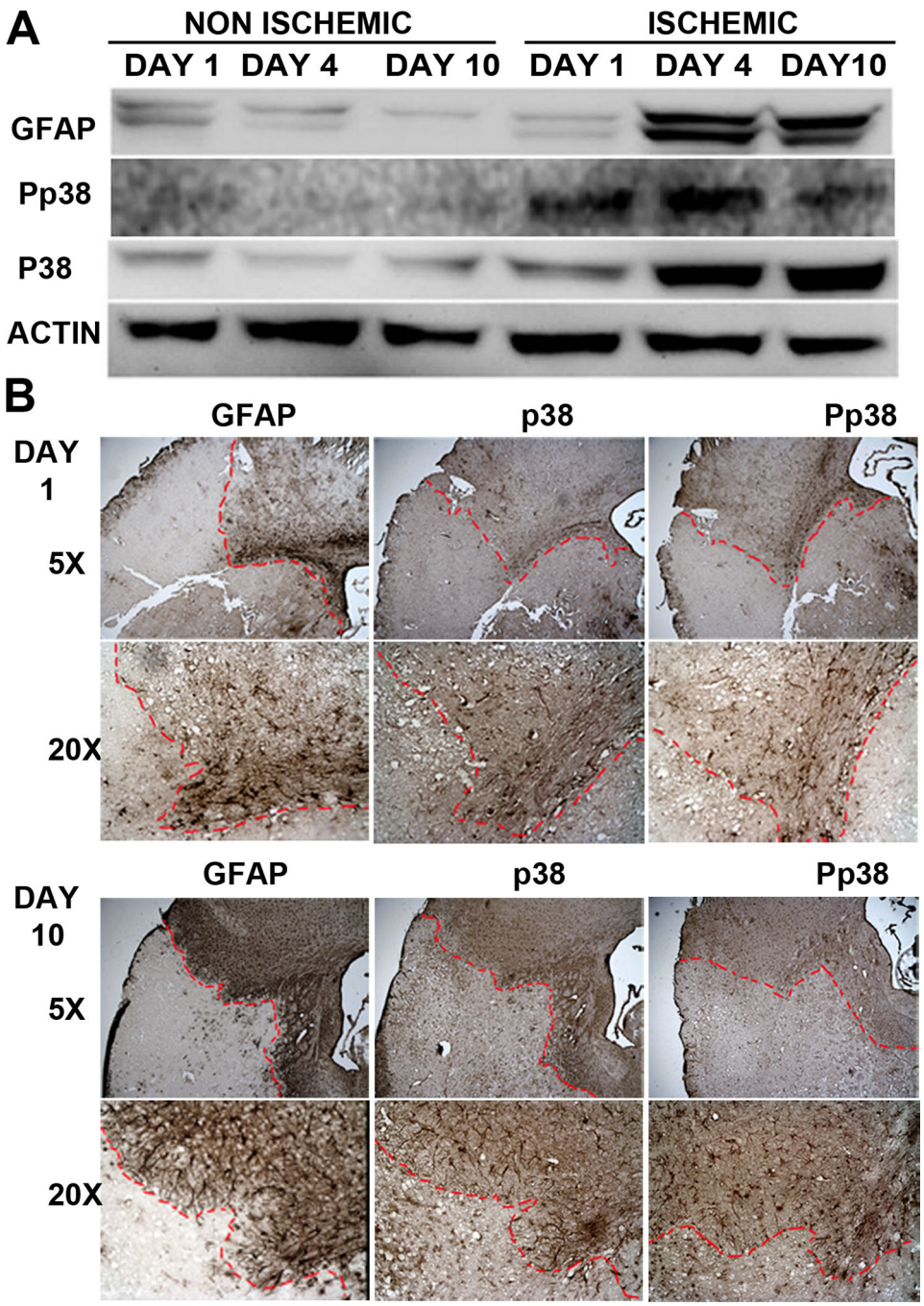

Figure 1. Increase of GFAP and p38 expression in the peri-infarct region after ischemic stroke

A. Representative Western blots demonstrated an increase of GFAP and p38 expression in the ischemic cortex at 4 and 10 days after transient focal cerebral ischemia in mice. **B**. Depicts are representative microscopic images (5× and 20× objective images) of GFAP, p38, and Pp38 immunohistochemistry at 1 or 10 days after transient focal cerebral ischemia in mice. Loss of GFAP, p38 and Pp38 staining was observed in the ischemic core. A time-dependent increase of GFAP, p38, and Pp38 expression was observed in the peri-infarct region at days 1 and 10 after stroke.

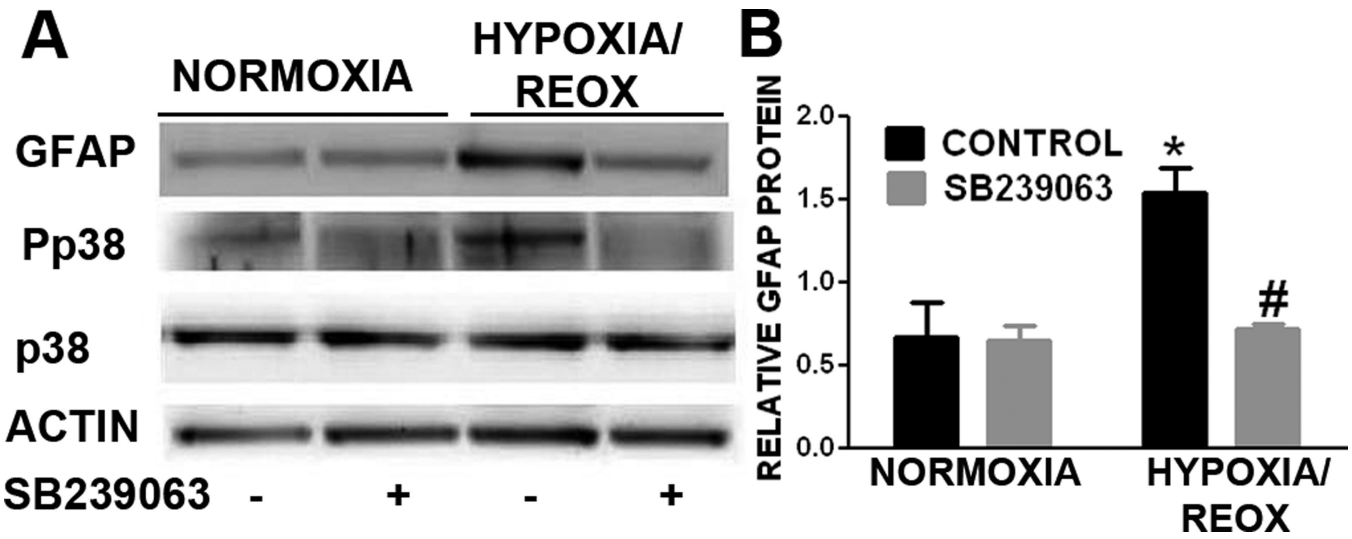

Figure 2. p38 MAPK inhibition attenuates OGD induced astrogliosis in primary astrocyte culture

A. Representative Western blots of primary astrocytes subjected to 3hr OGD and 24hr reoxygenation. A marked increase of GFAP and pp38 were observed after OGD/ reoxygenation. **B**. Quantitative analysis of GFAP Western blots demonstrated that OGD/ reoxygenation induced a significant increase in GFAP expression and p38 activation (pp38), which was significantly attenuated by SB239063 (10μg/mL). * $p < 0.05$ vs. normoxia control. # $p < 0.05$ vs. hypoxia control.

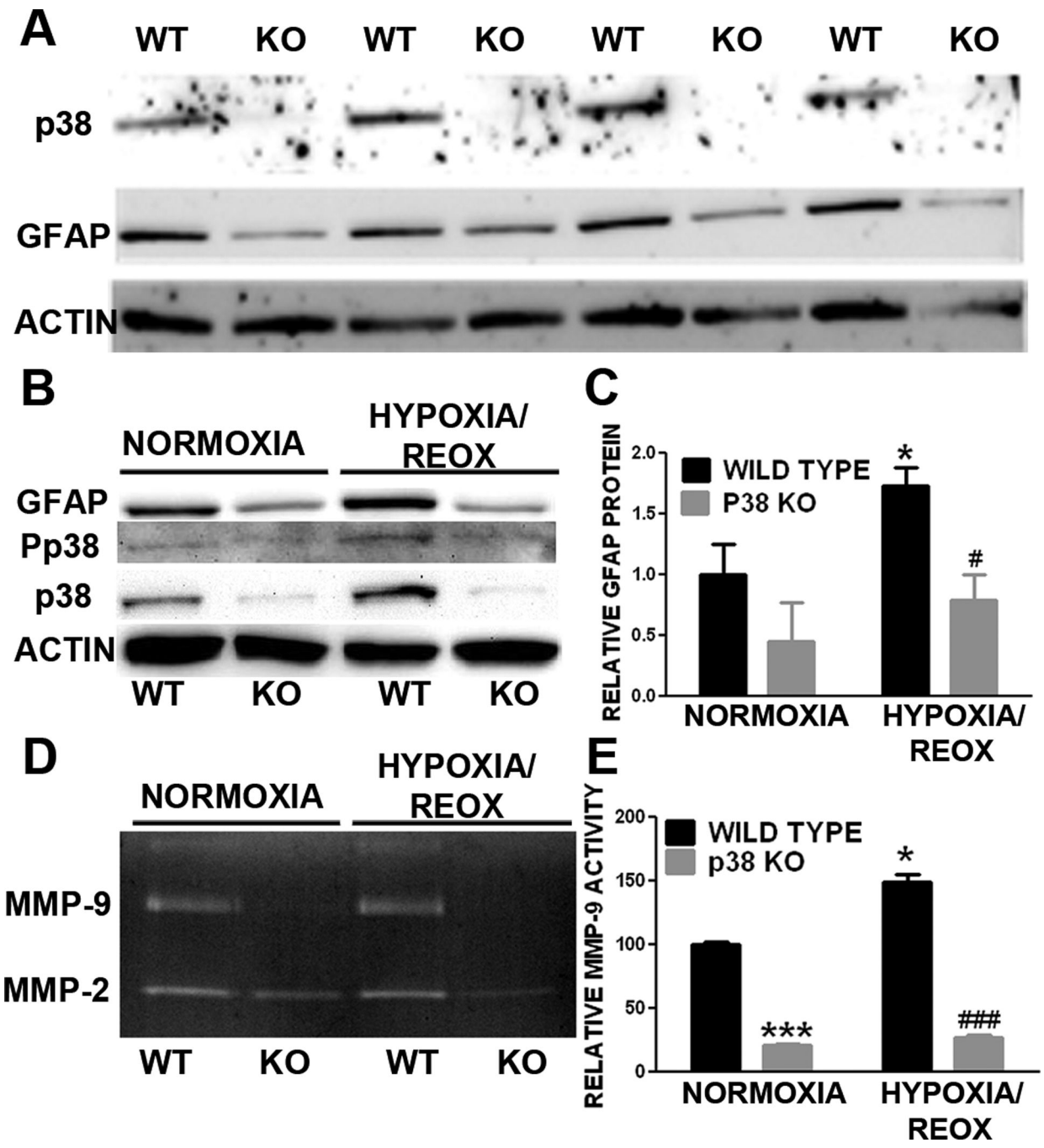

Figure 3. p38 MAPK knockout attenuates astrogliosis in primary astrocyte cultures

A. Depicts are representative Western blot of primary astrocyte cultures derived from wild type (WT) and GFAP/p38 knock out (KO) mice. Loss of p38 MAPK expression was associated with a marked reduction GFAP expression in primary astrocyte derived from GFAP/p38 knockout mice. **B**. Depicts are representative Western blots of primary astrocyte cultures subjected to normoxia or OGD/reoxygenation insult. Lower GFAP expression was observed in primary astrocyte culture derived from GFAP/p38 knockout mice under normoxic condition and subjected to OGD/reoxygenation insult. **C**. Quantitative analysis of

GFAP Western blots demonstrated that p38 MAPK knockout significantly decreased OGD/reoxygenation induced increase of GFAP expression in primary astrocyte cultures. * $p < 0.05$ vs. normoxia wild type. # $p < 0.05$ vs. hypoxia wild type **D**. Depict is a representative gelatin zymograph of media from wild type and GFAP/p38 knockout astrocyte cultures. **E.** Quantitative analysis of gelatin zymography demonstrated that p38 knockout significantly reduced MMP-9 activity under normoxia and after OGD/reoxygenation insult. ***$p < 0.001$ vs. normoxia wild type.. * $p < 0.05$ vs. normoxia wild type. ### $p < 0.001$ vs. hypoxia wild type.

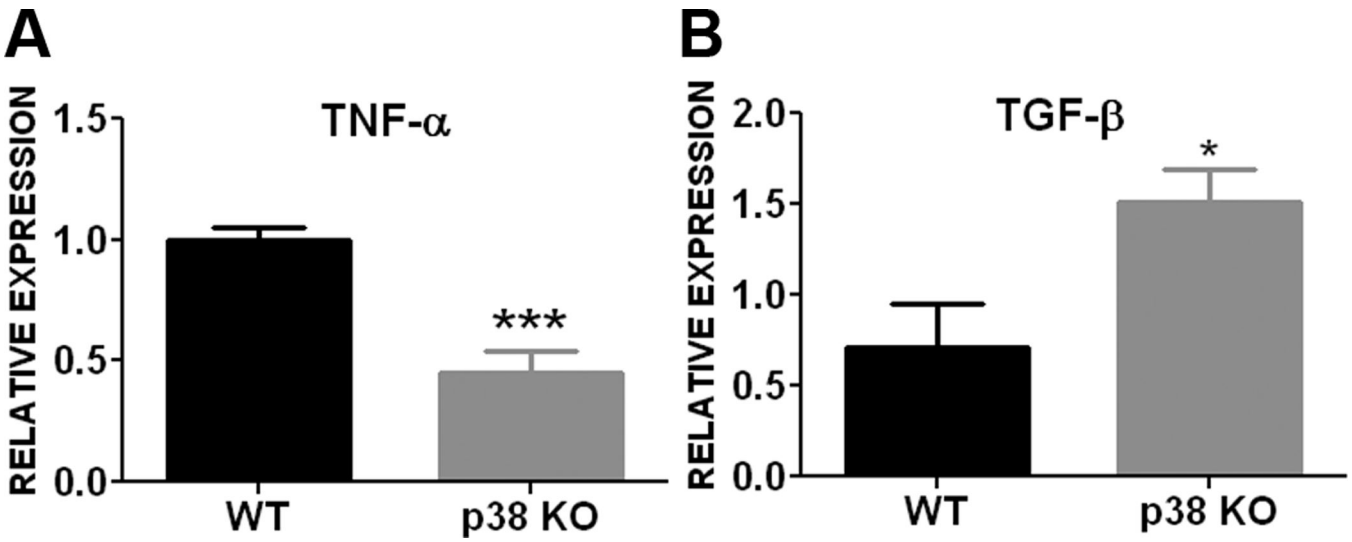

Figure 4. p38 MAPK inactivation alters cytokine expression in primary astrocyte cultures

A. Quantitative PCR analysis showed that conditional p38 knockout primary astrocytes had significantly lower mRNA expression of pro-inflammatory cytokine TNF-α compared to wild type astrocytes. **B**. Conditional p38 knockout astrocytes had significantly higher mRNA expression of anti-inflammatory cytokine TGF-β compared to wild type astrocytes. *** $p < 0.001$ vs wild type. * $p < 0.05$ vs. wild type.

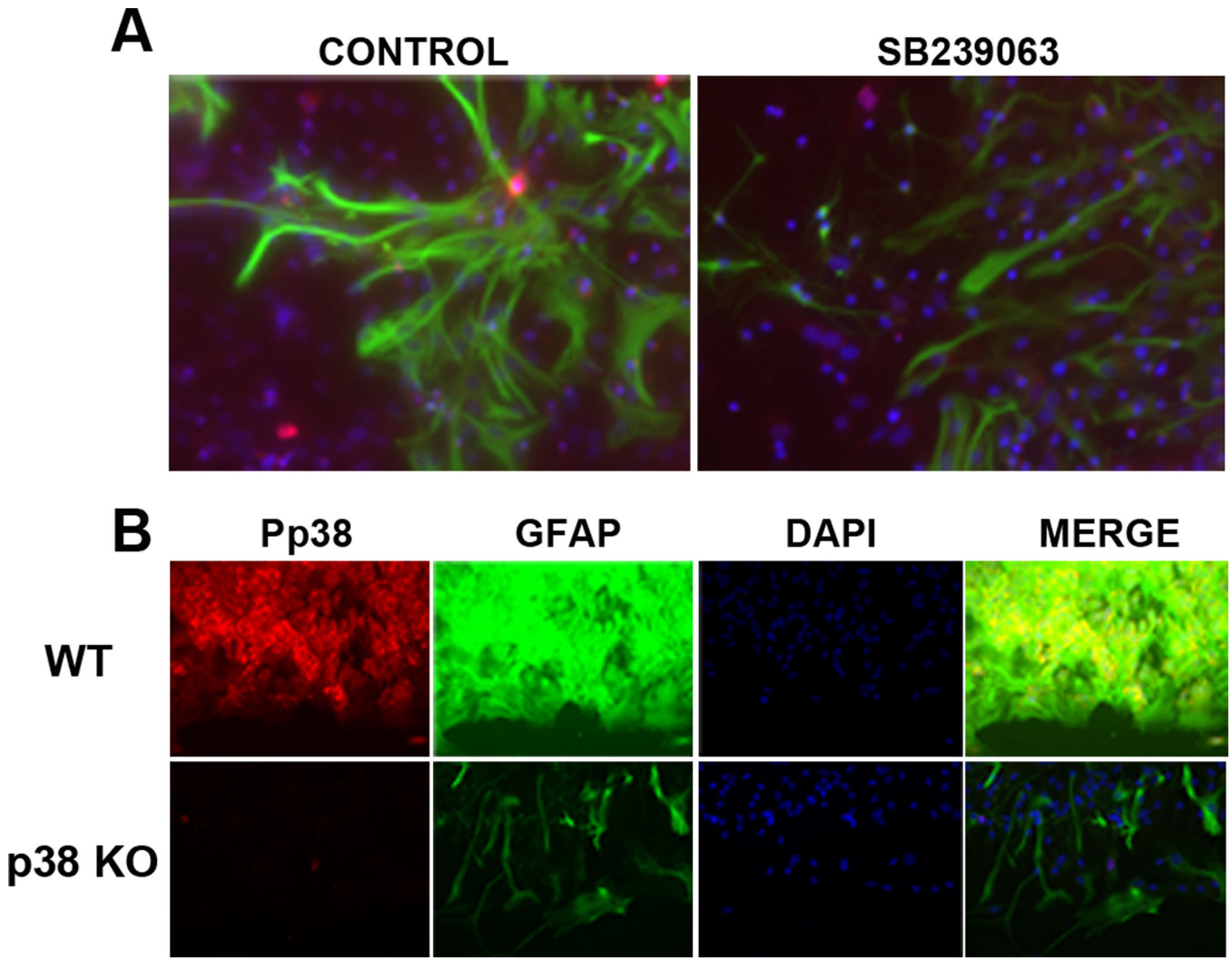

Figure 5. p38 MAPK inactivation attenuates scratch-induced astrogliosis in primary astrocyte cultures

A. Depicts are representative immunocytochemistry images of GFAP (green), Pp38 (red), DAPI (blue) in primary astrocyte cultures subjected to scratch injury. SB239063, a p38 inhibitor, markedly attenuates GFAP and Pp38 expression. **B**. Depicts are representative immunocytochemistry images of GFAP, Pp38, and DAPI in primary astrocyte cultures subjected to scratch injury. Scratch induced dramatic increase of Pp38 and GFAP expression in wild type astrocyte cultures which was blocked in primary astrocyte cultures derived from GFAP/p38 knockout mice.

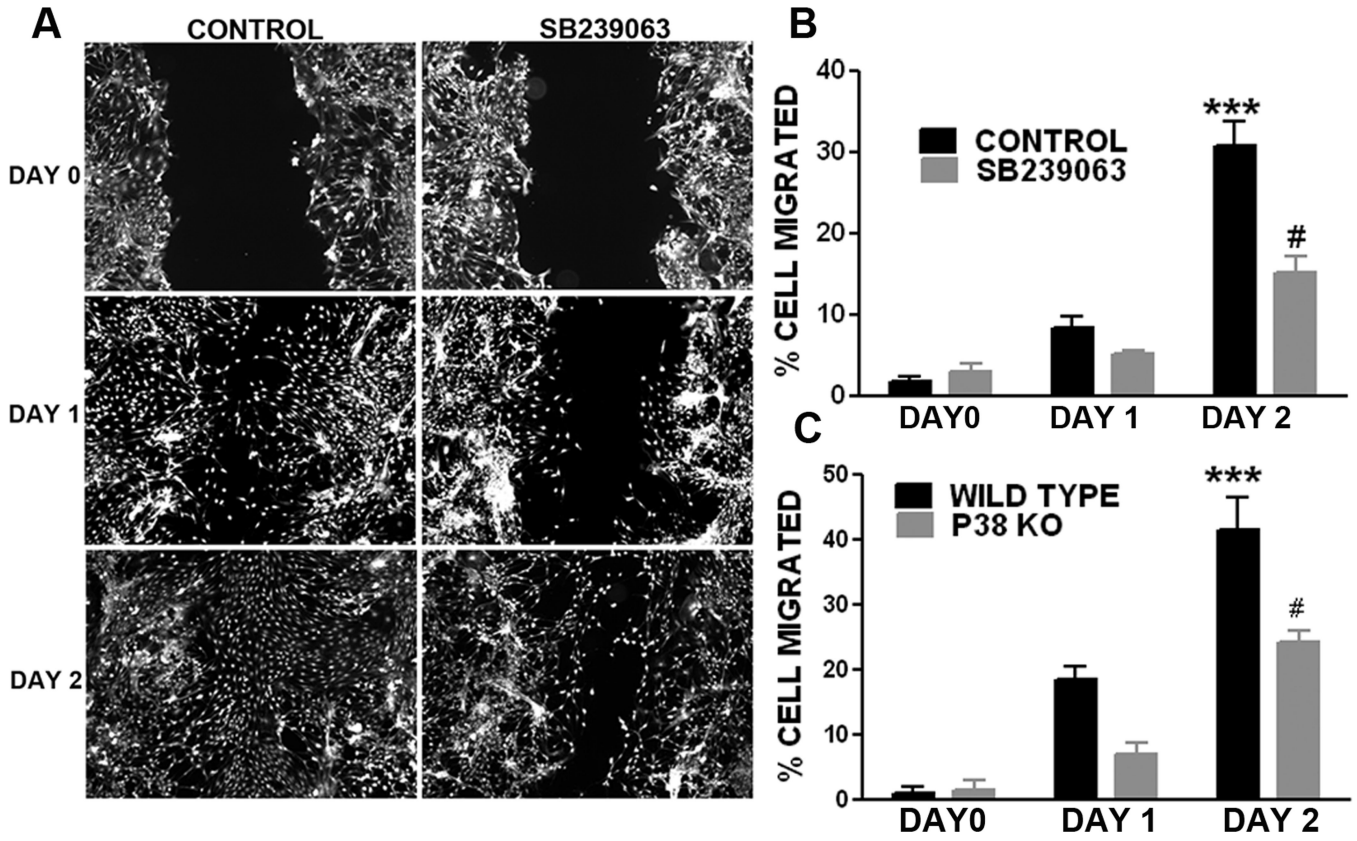

Figure 6. p38 MAPK inactivation attenuates wound healing in primary astrocyte cultures

A. Depicts are representative microscopic images of Calcein AM labeled astrocytes at day 0, 1, and 2 after scratch injury. SB239063, a p38 inhibitor, substantially slows down the healing process. **B**. Quantitative analysis of wound healing assay demonstrated that SB239063 significantly inhibits wound healing in primary astrocyte cultures. **C**. Quantitative analysis of wound healing assay in primary astrocyte cultures derived from wild type and GFAP/p38 knockout mice demonstrated that p38 knockout significantly inhibit wound healing. *** $p<0.001$ vs. day 1 WT, # $p<0.05$ vs. day 2 WT.

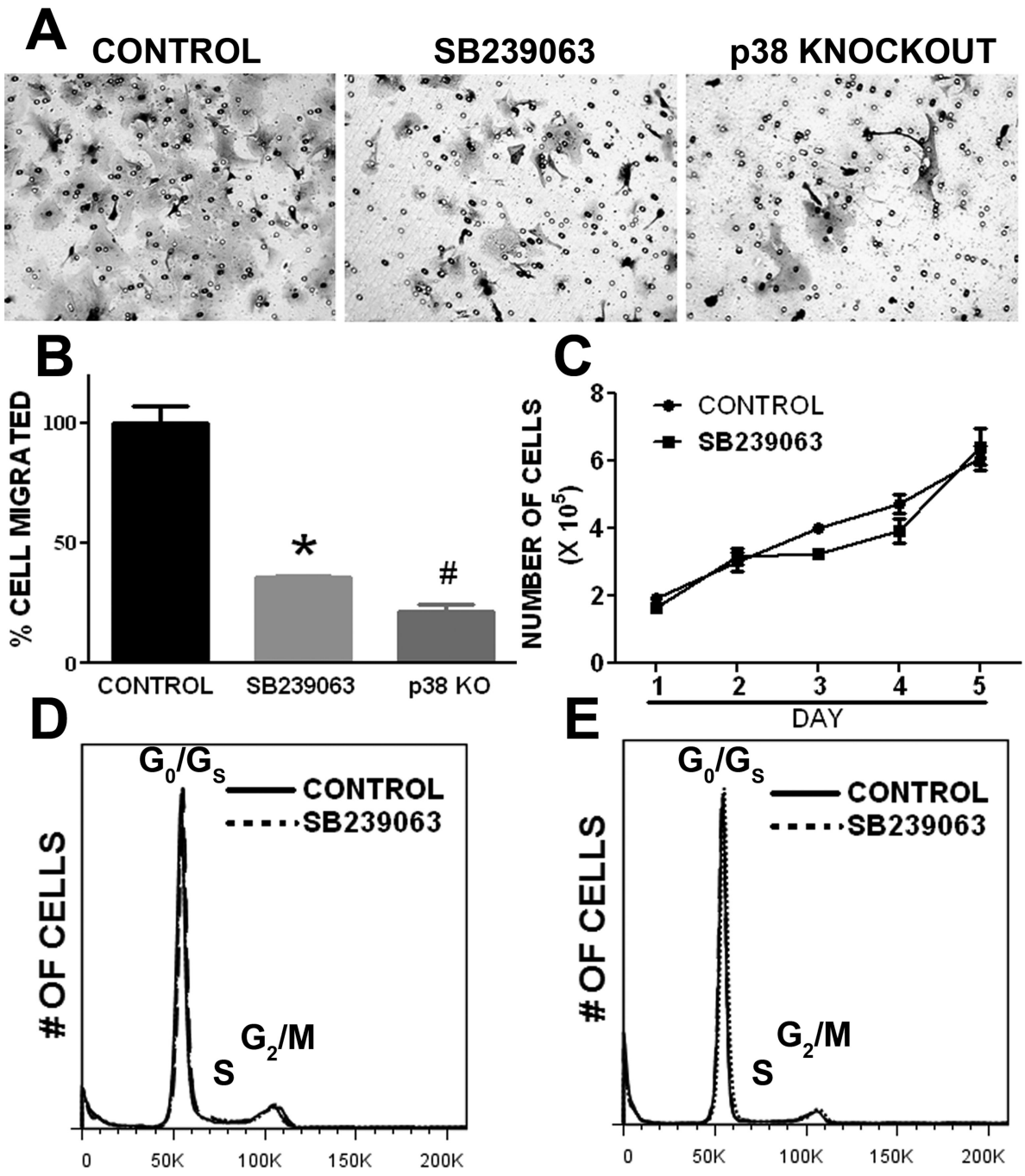

Figure 7. p38 MAPK inactivation inhibits primary astrocyte migration without affecting cell proliferation

A. Representative transwell assay images demonstrated that primary astrocyte migration was inhibited by p38 MAPK inhibitor, SB239063, and knockout. **B**. Quantitative analysis of transwell assay. * # $p<0.05$ vs. control. **C**. Growth curve assay of primary astrocyte with treatment of SB239063 or control. p38 MAPK inhibition did not affect primary astrocyte proliferation. **D** & **E**. Representative cell cycle analysis of primary astrocyte culture at day 1

and day 2, respectively, after treatment of SB239063 or control. p38 MAPK inhibitor did not affect cell cycle of primary astrocyte culture.

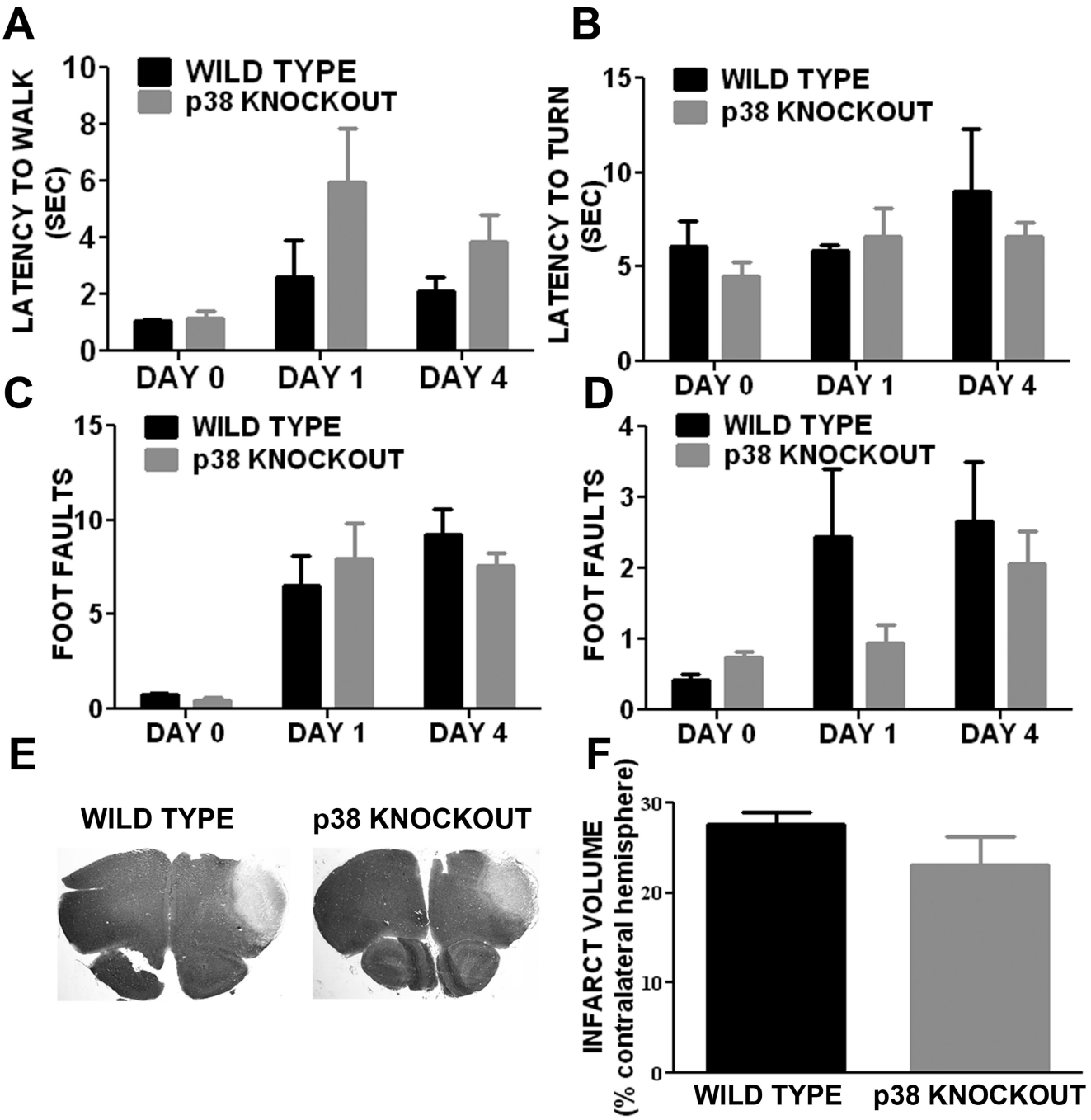

Figure 8. Astrocyte p38 MAPK knockout has no effect on motor function recovery and lesion volume at acute stage after permanent MCAO in mice

Results from behavioral studies performed before and on days 1, 4 after MCAO. **A.** Latency for walk initiation. **B.** Latency to turn and reverse direction. **C** & **D.** Foot faults made by fore paw (C) and hind paw (D), respectively, during ladder rung walking test. **E**. Representative image depicting the cresyl violet staining of wild type and GFAP/p38 Knockout mice brain sections. **F**. Quantitative analysis of infarct volume showed that there was no significant difference in infarct volume between wild type and GFAP/p38 Knockout mice.

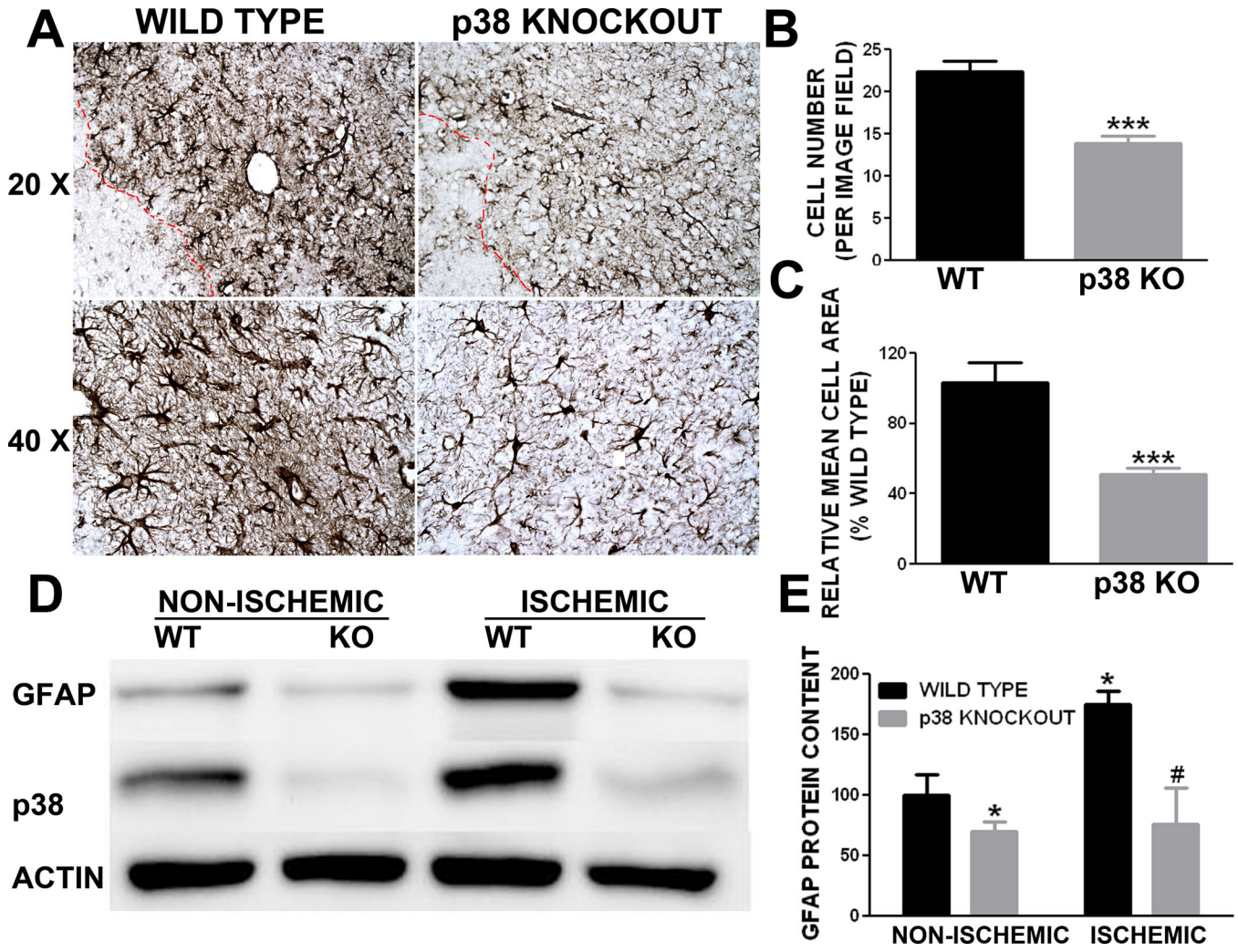

Figure 9. p38 MAPK knockout attenuated astrogliosis induced by permanent middle cerebral artery occlusion in mice

A. Depicts are representative GFAP immunohistochemistry images demonstrated that conditional knockout p38 in astrocyte attenuates astrogliosis at 4 days after stroke. **B**. Quantitative analysis of GFAP positive astrocyte number demonstrated that GFAP/p38 knockout mice have significant fewer astrocytes in the peri-infarct region compared to wild type controls at day 4 after ischemic stroke (*** $p<0.001$ vs. wild type). **C**. Quantitative morphometric analysis of GFAP positive astrocytes indicated that GFAP/p38 knockout mice have significantly smaller astrocytes in the peri-infarct region compared to wild type littermates at day 4 after ischemic stroke (*** $p<0.001$ vs. wild type). D. Depicts are representative Western blots of GFAP, p38 and actin from non-ischemic and ischemic cortex of wild type littermates and GFAP/p38 knockout mice. E. Quantitative analysis of GFAP Western blots demonstrated that GFAP/p38 knockout mice have significantly lower GFAP expression in both ischemic and non-ischemic hemisphere compared to wild type littermates (* $p<0.05$ vs. wild type non ischemic hemisphere. # $p<0.05$ vs. wild type ischemic hemisphere).